Astron. Astrophys. 341, 451–457 (1999)

ASTRONOMY
AND
ASTROPHYSICS

Interstellar reddening from the Hipparcos and Tycho catalogues

II. Nearby dust features at the NGP associated with approaching HI gas

J. Knude and E. Høg

Niels Bohr Institute for Astronomy, Geophysics and Physics, Juliane Maries Vej 32, DK-2100 København Ø, Denmark
(e-mail: indus@astro.ku.dk)

Received 24 September 1998 / Accepted 7 October 1998

Abstract. The Hipparcos and Tycho Catalogues offer an interesting possibility to study the local distribution of the interstellar reddening from the combination of data contained in the catalogues: Hipparcos parallaxes, Tycho $B-V$ and spectral and luminosity classification compiled from the literature, mainly the Michigan Catalogs.

In some cases the distances to intermediate velocity (IV) gas features may be estimated from positional coincidence between HI gas in narrow velocity intervals and E_{B-V} v. distance features extracted independently from the Hipparcos and Tycho Catalogues. Presently about $33\,000$ sight lines are available for interstellar studies.

Apart from the IV Arch the other possible dust counterparts are identified without a priori knowledge of the positions of the 21 cm gas with deviating velocities. Some features are revealed immediately in the E_{B-V} v. distance diagram for the north galactic cap. Color excesss $-$ distance data for $b > 60^\circ$ reveal two dust features at ≈50 pc and ≈300 pc with color excesses much larger than the average NGP reddening. We present circumstantial evidence that the distances of these features may pertain mainly to gas with intermediate negative velocity. The nearest NGP dust spike is sharply defined and may be related to a 21 cm feature with V_{lsr} in the range $[-37 \mid -27]\,\mathrm{km\,s^{-1}}$. The 300 pc feature may be related to three distinct hydrogen features: the edge of a $[-60 \mid -57.5]\,\mathrm{km\,s^{-1}}$ structure, and a fragmented loop with V_{lsr} between -30 and $-25\,\mathrm{km\,s^{-1}}$. These results indicate that high velocity gas may be local, a suggestion gaining ground since the discovery of low velocity bridges.

Another result is that gas to dust ratio along the sight lines at the positional associations are found to $N_H/E_{B-V} \lesssim 5\ 10^{20}\,\mathrm{cm^{-2}\,mag^{-1}}$, an order of magnitude smaller than the canonical value. If this implies depletion it is no wonder that interstellar absorption lines with velocities matching the IV gas have not been observed.

Since dust is predominantly destroyed by shocks in the warm neutral/ionized part of the interstellar medium and we discuss features with larger than normal dust/gas ratio the IV gas could be cold.

There is just an indication of a shell like structure between 30 and 50 pc where the proposed Perseus Superbubble is expected to be located between 50 and 80 pc.

Key words: ISM: clouds – ISM: dust, extinction – galaxy: solar neighbourhood

1. Introduction

The distance to high and intermediate velocity clouds have presented a challenge since their discovery. Their origin and their distance have been questioned. They are generally perceived as remote. There has, however, also been recent developments indicating that they, or gas related to them, may be even very nearby so that some of them in fact may constitute part of the local interstellar medium. Verschuur (1993) proposes a supershell model. Here the question really is about a supershell, originating in the Perseus arm and impacting the local interstellar medium. The distance to the near side of this interaction might be as small as 30 pc. Another line of evidence is the observation of low velocity bridges that seem intimately related to high velocity features, Pietz et al (1996). If the intermediate and high velocity gas have local imprints and if there is dust associated with this gas, studies of the continuum absorption resulting from the spatial distribution of the dust may possibly contribute to the determination of the distances to the HI structures with large velocities. Continuum studies can not provide identification from an identity of velocities as is possible from optical absorption line studies. A criterion is instead a positional match of a continuum absorption feature with a velocity structure. Such identifications are best performed at high galactic latitudes where things are simpler.

2. Hipparcos – Tycho data

As discussed by Knude and Høg (1998, herafter KH) the Hipparcos parallaxes, the Tycho colors and the spectral, luminosity classification, mainly from the Michigan Catalogs, allow the computation of a unique (distance, E_{B-V}) data set. The only change from KH is that we now include the LC IV stars, a further $2\,500$ sight lines are added to the sample. Their slightly larger luminosity further increases the samples penetrating power into more obscured regions at a given distance and the inclusion augments the number of sight lines at northern declinations where Michigan classifications are unpublished. We apply the LC V relation of Schmidt-Kaler (1982) also for LC IV. Justification for this may be found in the study of the $(B-V)$ colors of bright stars, $V \lesssim 6.5$, by Davidson, Scott Claflin and Haisch (1987) where a superposition of the $(B-V)$ − spectral type diagram for LC V and LC IV shows that these two classes share a common lower envelope, the intrinsic spectral type v. $(B-V)_0$ relation. A plot of the $\sim 2\,500$ LC IV stars from the Hipparcos and Tycho Cataloque together with the LC V $(B-V)_0$ relation from Schmidt-Kaler (1982) shows that the intrinsic relation matches the LC IV stars as well as the LC V ones.

It is of course a problem that the surface density of classified stars does depend on declination because the published Michigan catalogs are confined to $\delta < -12°$. Another problem is the rather bright magnitude limit of the Hipparcos Survey, the possible detections of dust features have acordingly a rather random nature. The completeness of the Hipparcos Survey (see ESA 1997 Volume 1 p. 131) depends on latitude and spectral type and ranges from about 7.5 to about 9.0. This means that a systematic study presently would be confined to southern declinations and to the volume within at most a few hundred pc. Parallaxes for these distances have a relative error typically better than 15–20% and the computed color excesses are estimated to be accurate to about 0.030 mag from fields with approximately zero reddening, depending on spectral type. See e.g. the distances between 70 and 170 pc in Fig. 4. Stars earlier than about K3 have more accurate color excess estimates than later types. Color excesses for LC V and IV are generally better than for LC III. See Fig. 1 of KH. The accuracy of individual color excesses is not crucial for the identification of the dust features, the presence of extinction jumps is more essential and may be seen if the discontinuity is larger than about 0.1 mag. The high precision of the distances is of course also important.

In the first place we do not attempt to locate the high and intermediate velocity gas by investigating the color excess distribution within regions recognized to contain this gas, Wakker and van Woerden (1997), since these confinements most often will also contain dust pertaining to features not related to the high and intermediate velocity structures and we are not able to make a distinction from the E_{B-V} v. distance diagram.

Our proposed identification is obtained completely from positional coincidences between the gas features and a dust feature, defined from independent criteria. We base our identifications on relatively large color excesses despite of the expectation that very little dust may be associated with deviant velocity features, see the discussion in the following section.

3. Optical dust at the galactic poles measured by Hipparcos − Tycho, a way into intermediate velocity features?

How can a color excess observation be associated with high and intermediate velocity gas at all since it contains no velocity information? First we consider the observational error of an color excess and compare it to the expected range of N_H associated with the high velocity (HV) and intermediate velocity (IV) gas. The best color excess measurements have an error $\sigma_{E_{b-y}} \lesssim 0.008$ mag corresponding to $N_H \approx 6\ 10^{19}\,\mathrm{cm}^{-2}$. A three sigma detection accordingly requires $N_H \approx 1.8\ 10^{20}\,\mathrm{cm}^{-2}$. With our present accuracy $3\sigma_{E_{B-V}} \approx 0.090$ corresponds to $4.8\,10^{20}\,\mathrm{cm}^{-2}$. Wakker (1991) has presented the column density distribution of the high velocity gas over the complete sky and the probability to encounter $2\ 10^{20}\,\mathrm{cm}^{-2}$ seems low, and such column densities are definitely not measured at high northern latitudes. Kuntz and Danly (1996) have presented an integrated contour map for $-90 < \mathrm{V}_{lsr} < -20\,\mathrm{km\,s}^{-1}$, $b > 0°$ gas. Intermediate velocity gas with $N_H \gtrsim 2\,10^{20}\,\mathrm{cm}^{-2}$ is only encountered for $b < 10°$. Since a halo origin of the HV and IV gas is among the possibilities there is no a priori expectation that the gas/dust ratio is standard. Wakker and Boulanger (1986) searched for infrared emission from HVCs with a negative outcome. Their conclusion was that either the HVC dust is cooler or the dust/gas ratio is a factor of 3 smaller than in low velocity clouds, see Sect. 7 for a discussion of the gas/dust ratio. Boulanger et al (1996) do find a tight 100 μm − 21 cm emission correlation at high galactic latitudes valid for the low velocity gas.

Grain destruction in interstellar shocks may also reduce the dust to gas ratio in HV and IV gas (Spitzer 1978). Table 3.2 of Spitzer demonstrates that the Na/Ca ratio varies with cloud velocity. Depletion could thus decrease with cloud velocity since relatively more grains are destroyed at larger velocities and the metals returned to the gas. Or the ionization balance is changed with cloud velocity thus not necessarily altering the depletion (Spitzer 1978). Grain destruction by shocks is most efficient in the warm neutral/ionized part of the interstellar medium with T $\approx 10\,000$ K and density $n_H \lesssim 0.25\,\mathrm{cm}^{-3}$ (Jones, Thielens and Hollenbach 1996). Destruction by grain−grain collisions are dominant for shock velocities $\leq 50-80\,\mathrm{km\,s}^{-1}$, typical IV gas velocities (Jones et al 1994).

The prospects for a detection of the dust counterpart of the deviant velocity gas seems bleak! Low columns and little dust are to be expected in the high and intermediate velocity features unless the temperature is very low in which case the dust would not have been observed at 100 μm or has been destroyed by interstellar shocks.

We will approach the problem in two ways. First we will concentrate on the high galactic latitudes where the matter distribution is simplest and search for conspicuous but "coherent" dust features. Secondly we will study the color excess distribution inside the intermediate velocity feature known as IV Arch (see Kuntz and Danly 1996).

The reddening at the galactic poles has caused much discussion over the years and may in fact show a rather complex distribution. Substantial amounts of reddening are present above b = 70° and some individual clouds are confirmed in the ultraviolet, optical and infrared, e.g. the Galactic cirrus cloud G251.2+73.3 with $A_V \approx 0.4$ (Haikkala et al 1995). The average reddening for $b > +70°$ is $E_{b-y} = 0.014$ but one third of the cap has $E_{b-y} > 0.030$ mag (Knude 1996). The conversion from E_{b-y} to E_{B-V} is $E_{B-V} = \frac{1}{0.74}\,E_{b-y}$.

Fig. 1 shows the polar cap $b > 60°$ as measured by Hipparcos − Tycho. The number of stars is small due to the reasons mentioned above. Nevertheless, the diagram reveals features which have not been noticed before, possibly because later stel-

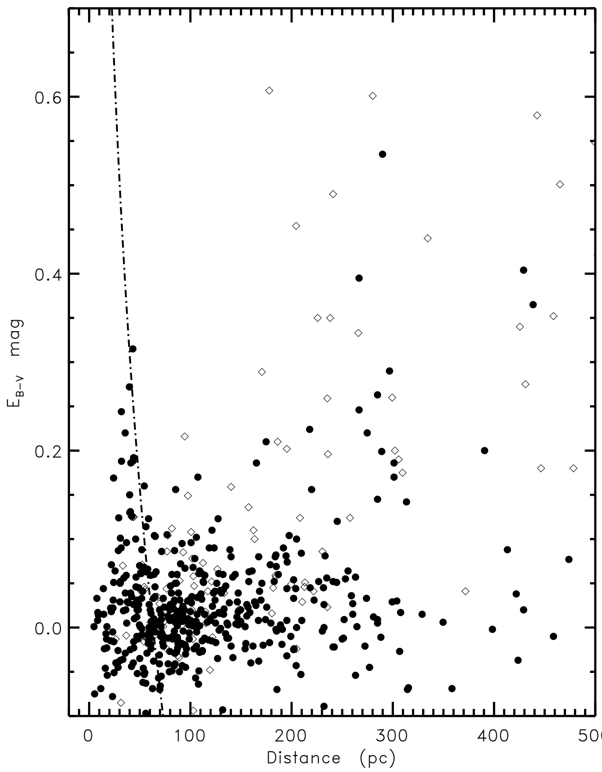

Fig. 1. E_{B-V} versus distance for $b > 60°$. LC V •, LC IV ⋄. Curve outlines maximum detectable E_{B-V} for V_{lim} = 9.0 and M_V = 5.0

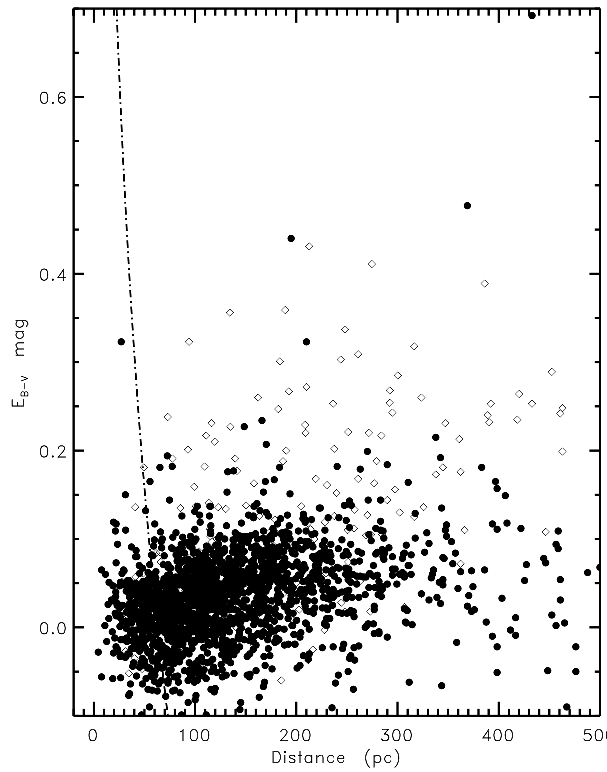

Fig. 2. E_{B-V} versus distance for $b < -60°$. LC V •, LC IV ⋄. Curve outlines maximum detectable E_{B-V} for V_{lim} = 9.0 and $M_V = 5.0$

lar types than previously are included, opening for measurements of very nearby dust.

Why do we consider the high latitudes? Inspecting the Galactic HI distributions in interesting velocity intervals in the Leiden/Dwingeloo Survey of Galactic Neutral Hydrogen, Hartmann (1994), one notices the presence of rather isolated structures which are sharply defined at moderately negative velocities at high northern and southern latitudes. The 21 cm intensity distribution for IV gas seems rather inhomogeneous and it would be difficult to prepare an observing programme probing E_{B-V} of the brightest features, e.g. with velocities between -45 and -40 km s^{-1} above 60°, Hartmann (1994) Plates 4.37, 4.38. The brightest features, supposed to produce the largest reddening, have very small solid angles and how should one preselect the magnitude range to be observed when the distance is completely unknown? A feature that might be detected is the strong contrast seen for $60° < b < 80°$ and l between 100° and 120° and 240° and 260° respectively, Hartmann (1994) Plates 4.27, 4.28. If this contrast is due to a tangential sight line to a shell like structure it might be associated with some reddening. Plates 4.43 and 4.44 valid for the V_{lsr} range $[-30 \mid -25]$ km s^{-1} display an almost complete circle centered on (l, b) = (140,0) and with an extension in latitude from $-80°$ to +80°. The best approach to search for a dust counterpart of such gas could thus be to look at the polar caps. Returning to Fig. 1 we notice an extinction jump characterized by distances less than 60 pc and $E_{B-V} > 0.09$ mag. This is an unusual feature as the similar diagram for the south polar cap in Fig. 2 shows. The complete Hipparcos – Tycho dwarf sample contains only 140 stars within 60 pc and with $E_{B-V} > 0.09$ mag. The number of stars in the $\sim$50 pc spike is so large that it is probably not a statistical feature. The stars located in this spike are bright and mostly late type F and early type G. It contains no LC IV stars and only one LC III (not shown in Fig. 1). The curve in Fig. 1 displays the maximum detectable color excess for a given distance for stars with M_V = 5.0 and V_{lim} = 9.0, values representative for the stellar types noted in the spike and the Hipparcos survey has $V_{lim} \approx 9$ for spectral types earlier than G5 at these latitudes. The spike may accordingly be an artefact, but not the nearness of the onset of the large color excesses. The Hipparcos – Tycho data are biased in the sense that large color excesses are only measurable at short distances. The distance for the onset of a large reddening is correct if it is found shortwards of the $E_{B-V}(max)$ curve. The large color excesses measured at smaller distances than indicated by the curve are real but the Hipparcos survey limit does not allow the systematic inclusion of stars more remote and/or more reddened than indicated by the $E_{B-V}(max)$ curve. But we may conclude that a tiny fraction of the stars with $b > 60°$ located within ≈ 50 pc have a color excess $E_{B-V} > 0.090$ mag. The cap below $b = -60°$ does not display a similar spike, Fig. 2. The other noticeable feature in Fig. 1 is the presence of reddenings between 0.1 and 0.6 mag for distances in the range $\approx 200 - \approx 300$ pc. These reddenings are measured both by LC V and LC IV stars.

Fig. 1 further indicates that the polar reddenings at distances beyond 200 pc almost fall in two distinct groups. A low redden-

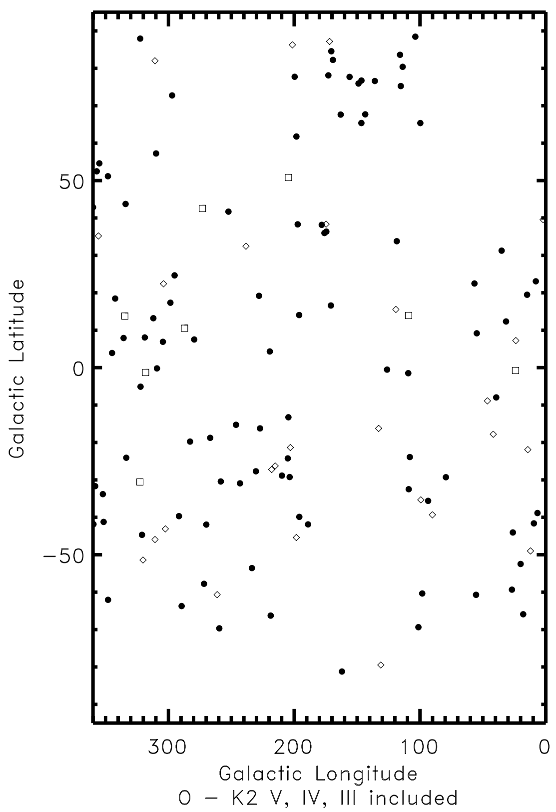

Fig. 3. Location of sight lines which measure $E_{B-V} > 0.090$ mag within 60 pc. LC V •, LC IV ◇, LC III □

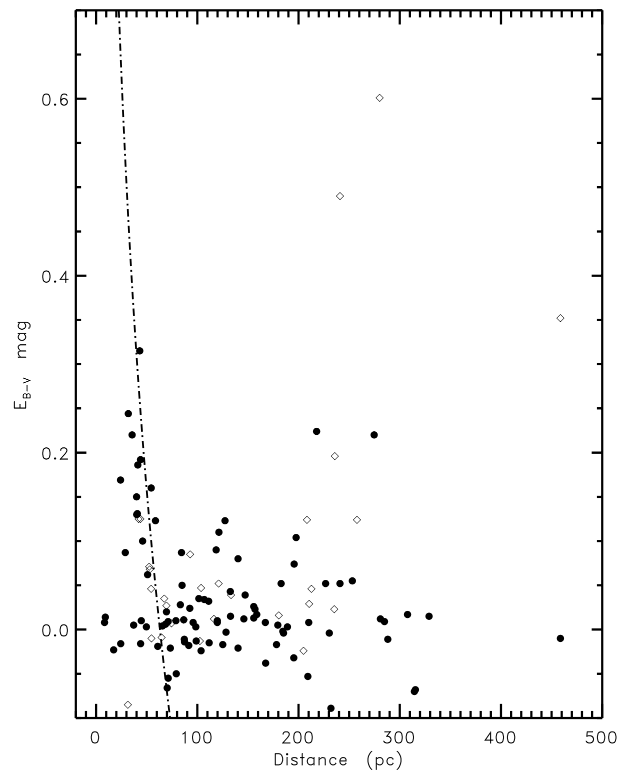

Fig. 4. E_{B-V} versus distance for $75 < b < 90°$ and $90 < l < 210°$. This diagram includes spectral types no later than K2. LC V •, LC IV ◇. Curve outlines maximum detectable E_{B-V} for $V_{lim} = 9.0$ and $M_V = 5.0$

ing measuring $E_{B-V} \approx 0$ ±0.03 mag and the high reddening with $E_{B-V} > 0.1$ mag. Apparently there are visual absorptions in this distance slot and with $b > 60°$ approaching $A_V = 2$ mag, quite unexpected considering previous discussions of the NGP reddening. Also noticed in Fig. 1 is that the separation in a low and high reddening part persists beyond the 300 pc, and the less reddened part is measured almost exclusively by the less luminous LC V stars. We have not plotted LC III in Fig. 1. Their inclusion will not alter the appearence of the 50 pc spike and the large excesses between 200 and 300 pc, but they will smear the reddening separation beyond 200 pc due to their larger color excess error.

4. Counterparts to the 50 pc NGP dust spike

Does the ∼50 pc $E_{B-V} \gtrsim 0.09$ feature recognized for $b > 60°$ have any counterparts at latitudes below 60°? Fig. 3 is an all sky map of the sight lines meeting the two criteria: distance less than 60 pc and color excess larger than 0.09 mag. The figure includes LC III, IV, V but only spectral types earlier than K3 in order to have the most accurate color excesses. Quite a number of sight lines meet these criteria but the largest density is found for longitudes between 100 and 200° and latitudes above 70°, and therefore this area is studied in Fig. 4.

In Fig. 4 we display the E_{B-V} v. distance diagram for the region $75 < b < 90°$ and $90 < l < 210°$. This tiny area contains both the two conspicuous features we noticed in Fig. 1: the spike at ∼50 pc and the large excesses between 200 and 300 pc. The striking thing is that these sight lines are concentrated to a very narrow latitude range so they might in fact fit some of the intermediate velocity features measured at high northern latitudes. We have compared the sight lines of Fig. 4, $b > 75°$ and $E_{B-V} > 0.09$ mag, with Hartmann (1994) and find an extraordinary fit to his Plate 4.42, the sky image integrated for $-32.5 < V_{lsr} < -30.0$ km s^{-1} (see Fig. 5). Even the few points near the SGP fall on the arch like structure as do the points with l exceeding 200° between latitude 50 and 60.

The points just below the $[-32.5 \mid -30.0]$ arch in Fig. 5 are located on the arch with the velocity $[-42.5 \mid -40.0]$ km s^{-1}. Of the 48 points in Fig. 5, confined to the longitude range from 90° to 210°, more than 50% are located on the almost complete arch noticable in the $\gtrsim$10 km s^{-1} wide velocity range $[-42.5 \mid -30.0]$ km s^{-1} (not shown). Is it a coincidence that stars selected being closer than 60 pc and with $E_{B-V} > 0.090$ and with l between 90 and 210° have a positional association with the intermediate velocity 21 cm gas? If not the IV gas could be closer than 60 pc.

5. Counterparts to the 200–300 pc NGP dust spike

The positional identification of this feature is not unigue. The sight lines may be matched to two features with different velocities. About 30 sight lines are located along the almost com-

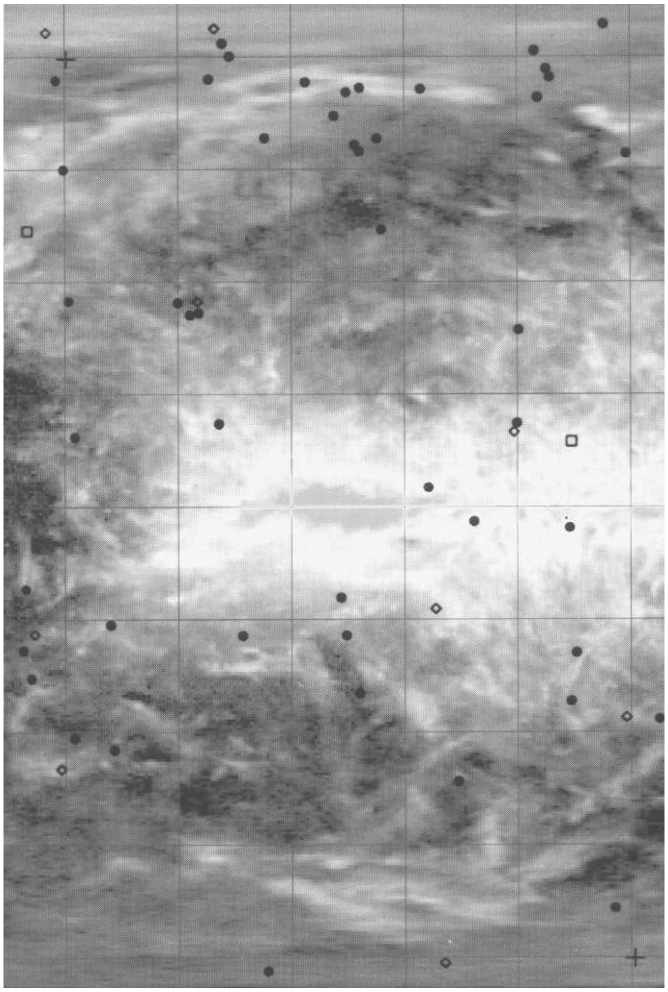

Fig. 5. Location of sight lines which measure $E_{B-V} > 0.090$ mag within 60 pc in the longitude range from 90 to 210°. LC V •, LC IV ⋄, LC III □. The overlaid $[-32.5 \mid -30.0]\,\mathrm{km\,s^{-1}}$ 21 cm data are from Hartmann(1994). The 21 cm intensity scale has been manipulated to enhance the low intensity features. The two + signs are located at (l, b) = (100,-80) and (200,+80) in the lower right and upper left corner, respectively

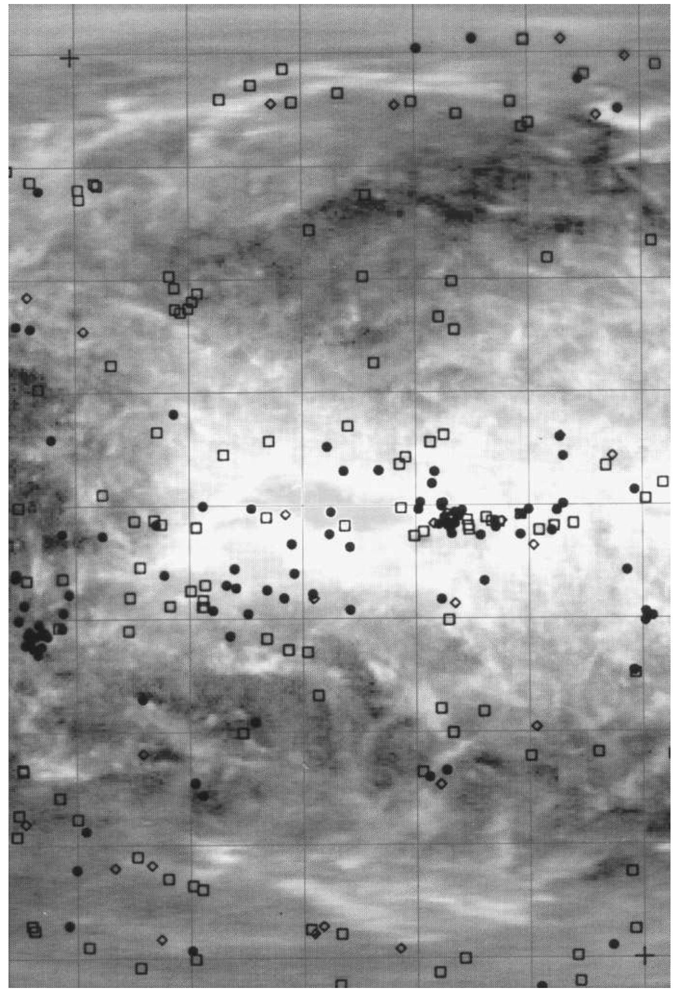

Fig. 6. Location of sight lines which measure $E_{B-V} > 0.10$ mag for the distance slot from 200 to 300 pc in the longitude range from 90 to 210°. LC V •, LC IV ⋄, LC III □. The sky image integrated between $[-27.5 \mid -25.0]\,\mathrm{km\,s^{-1}}$ is superposed. For this diagram we also searched the Catalogue for K3 − M9 stars. The 21 cm intensity scale has been manipulated to enhance the low intensity features. The two + signs are located at (l, b) = (100,−80) and (200,+80) in the lower right and upper left corner, respectively

plete circle present in the $[-30.0 \mid -25]\,\mathrm{km\,s^{-1}}$ range, Plates 4.43 and 4.44 Hartmann (1994). The overlay of Plate 4.44, $[-27.5 \mid -25.0]\,\mathrm{km\,s^{-1}}$ is shown in Fig. 6. Again we notice that the identification includes sight lines outside the $b > 60°$ zone where the 200–300 pc feature was first noticed. Fig. 2 also shows that a spike in this distance range may be present at the SGP. The lines of sight on the arch at the SGP (lower left of Fig. 5) is close to the northern limit of the Michigan Catalogs and the emptiness of the area just to the north of the southern part of the arch may accordingly be an artefact. The northern part of the $[-30.0 \mid -25.0]$ arch (not shown here) is located at systematically lower latitudes than the northern part of the $[-32.5 \mid -30.0]$ arch (Fig. 5), only a few degrees but significantly. The nearby arch (50 pc) thus has a velocity slightly more negative than the $[-30.0 \mid -25.0]$ arch at 200–300 pc, but a larger radius. An interpretation of these sizes, velocities and distances seems difficult.

The identification of the remaining high latitude sight lines pertaining to the 200–300 pc slot is proposed in Fig. 7, the $[-67.5 \mid -65.0]\,\mathrm{km\,s^{-1}}$ integrated sky image. A small group of stars is located along a very sharp edge in the upper right, in fact all but two of the stars in the upper right part of Fig. 7 matches the $[-67.5 \mid -65.0]$ edge exactly. Some of the sight lines represented in the 200–300 pc dust spike may be associated with gas at the most negative end of the intermediate velocity range, the usual division between high and intermediate velocity gas is at $-90\,\mathrm{km\,s^{-1}}$.

6. Search for dust counterparts to the IV Arch

Some of the IV features in fact have such well defined shapes and cover such large areas and are at such high latitudes that a comparison to the Hipparcos - Tycho reddening/distance pairs

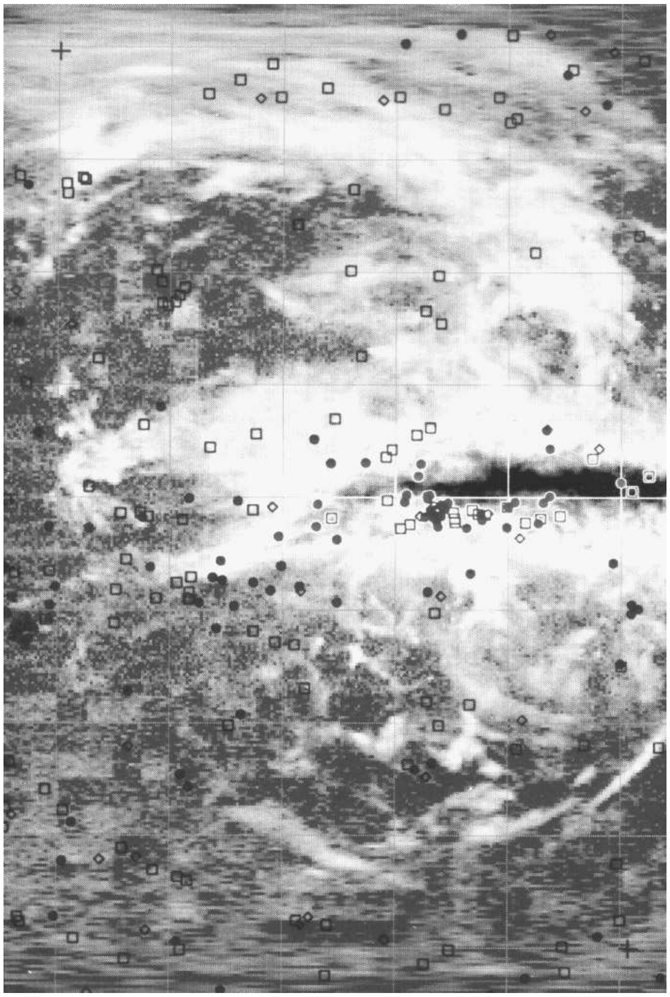

Fig. 7. Location of the same sight lines as in Fig. 6 which measure $E_{B-V} > 0.10$ mag for the distance slot from 200 to 300 pc in the longitude range from 90 to 210°. LC V •, LC IV ⋄, LC III □. The sky image integrated between $[-67.5 \mid -65.0]$ km s^{-1} is superposed. For this diagram we also searched the Catalogue for K3 − M9 stars. The 21 cm intensity scale has been manipulated to enhance the contrast between the low intensity emission at the high northern latitudes and the areas without emission. The two + signs are located at (l, b) = (100,−80) and (200,+80) in the lower right and upper left corner, respectively

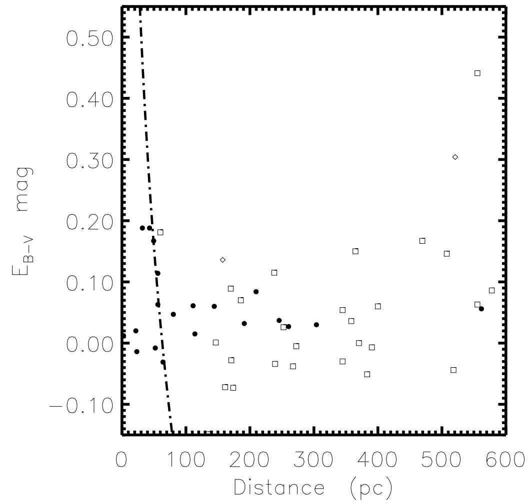

Fig. 8. Color excess v. distance for the region $140 < l < 190°$, $65 < b < 70°$ where the densest part of the IV Arch is located, spectral types later than K2 are included. The curve indicates the maximum detectable E_{B-V} with the limiting magnitude of the Survey part of the Hipparcos Catalogue

could be of interest. The IV Arch is such a feature as may be seen in Kuntz and Danly (1996). We have chosen to study the IV Arch in the velocity range from -100 to -80 km s^{-1}, see Kuntz and Danly Fig. 2, Plate 19 for the location on the sky. We have searched the $65 < b < 70°$, $140 < l < 190°$ part of the Hipparcos − Tycho Catalogue for stars. This area covers most of the IV Arch in the chosen velocity interval and contains 3–4 of its densest clumps. Fig. 8 displays the color excess v. distance diagram. There is only a small number of stars due to the northern location. But we notice a group of 4 stars closer than ≃60 pc and with $E_{B-V} > 0.160$ mag, implying $A_V > 0.5$ mag. It happens that the sight lines to these four stars form a small bundle with longitude ranging from 143.5 to 149.9 and latitude in the narrow range from 65.4 to 67.7. Distances are between 32 and 60 pc. Spectral types are K0 and K2. The average reddening is 0.181±0.010 mag. As Fig. 8 shows these large excesses are just included in the sample with the limiting magnitude of the Hipparcos Survey. There are three indications that this small blob of interstellar material may be connected with the IV Arch, two positional associations and one physical. If we compare our mean position (l, b) = (145°,+66°) to Fig. 8 of Kuntz and Danly we see that this clump is located just on a protrusion of the N_H = 3.2 10^{19} cm^{-2} contour of the $[-90 \mid -20]$ km s^{-1} gas, almost at the center of the void of low velocity gas. The second positional association is that the (145°, 66°) feature falls right on the ridge line of the IV Arch in Fig. 4 of Kuntz and Danly. The third part of the circumstantial evidence for an association is the gas to dust ratio. As mentioned $\langle E_{B-V} \rangle$ = 0.181±0.010 mag. If we assume the cloud is part of the IV Arch E_{B-V}/N_H = 3.2 10^{19}/0.181 = 1.7 10^{20} cm^{-2} mag^{-1}, but if we assume instead it is related to the low velocity gas E_{B-V}/N_H = 5.6 10^{19}/0.181 = 3.1 10^{20} cm^{-2} mag^{-1}. The N_H column densities are from Kuntz and Danly, Fig. 8. Combining the low and intermediate velocity gas will bring the ratio up to 4.9 10^{20} cm^{-2} mag^{-1}. We could also use the total column density for all velocities from Stark et al (1992) of 9 10^{19} cm^{-2} at (145,66) again resulting in a ratio 5 10^{20} cm^{-2} mag^{-1}. The small high - reddening region contains another 5 stars between 150 and 400 pc with an average color excess $\langle E_{B-V} \rangle$ = 0.038 mag which for the same gas column gives a ratio 2.4 10^{20}. The canonical ratio from Bohlin (1975) is 5.4 10^{21}. The gas/dust ratio is unusual in this direction and the gas to dust ratio for the (l, b) = (145°, 66°) feature is accordingly down with at least an order of magnitude. The conclusion of Wakker and Boulanger (1986) was that either the high velocity dust is cold or the dust/gas ratio is low by a factor of three. The (145,66) feature has a dust/gas ratio that is high by almost a factor of ten. This would

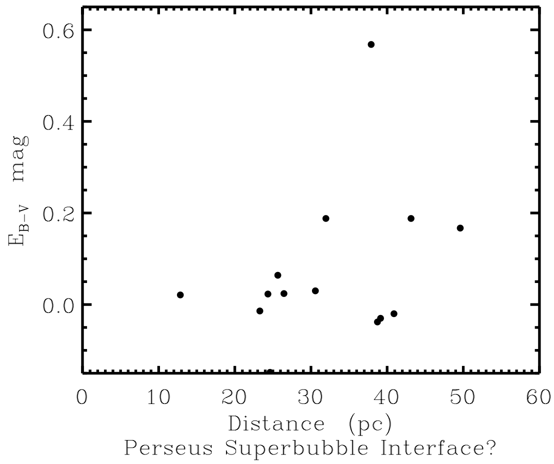

Fig. 9. Parallax limit in search 20 mas. Color excess v. distance for the region $140 < l < 160°$, $50 < b < 70°$ where the superbubble interface is expected at a distance 50–80 pc, Verschuur (1993). There are no LC IV and III stars resulting from the search

indicate that the (145,66) feature could be cold. So we may have observed a cold feature in the $[-100.0 \mid -80.0]$ km s^{-1} range.

With a standard E_{B-V}/A_V ratio the (145,66) feature would have $A_V \lesssim 0.5$ mag and might be detectable in CO measurements. In a survey of molecular gas at high northern latitudes Hartmann, Magnani and Thaddeus (1998) did not observe anything at the (145,66) position, but perhaps their grid was too coarse, two known molecular clouds (G107.4+70.9, G211+63) were missed at latitudes above 60°.

We might mention another coincidence. The sight lines within 60 pc above b = 75° and with $E_{B-V} > 0.09$ mag, Fig. 4 and Fig. 5, which we identified with $[-32.5 \mid -30.0]$ gas, run parallel to the IV contours of 1.8 10^{19} and 3.2 10^{19} cm^{-2} almost exactly. These directions display gas/dust ratio less than 2.0–3.6 10^{20}, also uncomfortably low. These sight lines are located in the IV Spur and IV Arch overlap.

7. Discussion

Distances to HV and IV gas are much debated, but we suggest a very local location for some of the IV gas. The velocity of the interstellar matter bridges between low and high velocity gas is partly based on identical arguments, Pietz et al (1996), but do of course measure the velocities bridging the high and the low velocity gas, an option not open for the color excess − distance data alone. The presence of IV gas within 60 pc and 200–300 pc, respectively, should of course be confirmed by observations of interstellar lines for the small number of stars defining the positional association. But will this be possible? The very odd gas/dust ratio noticed for these features might suggest that a considerable depletion is present. This could in fact explain why no absorption lines have been noticed in nearby stars in the direction of IV clouds. Verschuur (1993) proposes a super bubble originating in the Perseus arm causing the IV and HV gas in the direction $l \approx 145°$ and $b \approx 60$–$70°$ interstellar absorption lines may not be observable at the deviating velocities in nearby stars because the metal gas could be separated from the hydrogen gas during the kpc long passage from the Perseus arm. As discussed above the absent interstellar lines might be caused by an abnormally large depletion as in the (145,66) feature. Without the interference of Loop III Verschuur's model proposes that the supershell is at 30 pc in the plane for l = 147°.

Loop III does not interfere above $b = 50°$. In the region (l, b) = (140–160, 50–70) we searched the catalog for stars within 50 pc, the result is shown in Fig. 9. The stars in fact only occupy the latitude region from 52° to 67°. The three almost constant excesses pertain to the (145,66) feature. The largest excess is measured for an F4V star. The diagram contains, admittedly, very few sight lines but the straight forward interpretation is that we measure no interstellar matter out till ≈30 pc where a shell may be encountered. In this region the Perseus super bubble interface is proposed to be located in the distance range from 50 to 80 pc, see Verschuur (1993) Fig. 8(b). Is this near distance match a coincidence?

8. Conclusions

We have noticed positional coincidences between large color excesses and intermediate velocity gas at high northern latitudes and that the gas/dust ratio is an order of magnitude lower than normal in the (l, b) = (145,66) feature which may be connected with the IV Arch. Furthermore, the relatively low gas presence may help explaining why no interstellar absorption lines have been observed at intermediate velocities in nearby stars. The presence of a shell like structure at 30–60 pc coincides with the expectation for the Perseus Superbubble.

References

Bohlin R.C. ApJ 200, 402
Boulanger F., Abergel A., Bernard J.-P., et al., 1996, A&A 312, 256
Davidson G.T., Scott Claflin E., Haisch B.M., 1987, AJ 94, 771
ESA 1997, The Hipparcos and Tycho Catalogue 1997, ESA SP-1200
Haikkala L.K., Matilla K., Bowyer S., et al., 1995, ApJ 443, L33
Hartmann D., 1994, The Leiden/Dwingeloo Survey of Galactic Neutral Hydrogen. Thesis Sterrewacht Leiden
Hartmann D., Magnani L., Thaddeus P., 1998, ApJ 492, 205
Jones A.P, Thielens G.G.M., Hollenbach D.J., McKee C.F., 1994, ApJ 433, 797
Jones A.P, Thielens G.G.M., Hollenbach D.J., 1996, ApJ 469, 740
Knude J., 1996, A&A 306, 108
Knude J., Høg E., 1998, A&A 339, in press (KH)
Kuntz K.D., Danly L., 1996, ApJ 457, 703
Pietz J., Kerp J., Kalberla P.M.W, et al., 1996, A&A 308, L37
Schmidt-Kaler T., 1982, Landolt-Börnstein VI 2b, 1
Spitzer L., 1978, Physical Processes in the Interstellar Medium. Wiley, New York
Stark A.S., Gammie C.F., Wilson R.W., et al., 1992, ApJS 79, 77
Verschuur G.L., 1993, ApJ 409, 205
Wakker B.P., 1991, A&A 250, 499
Wakker B.P., Boulanger F., 1986, A&A 170, 84
Wakker B.P., van Woerden H., 1997, ARA&A 35, 217